

The quenching and survival of ultra-diffuse galaxies in the Coma cluster

C. Yoizin^{*} and K. Bekki^{*}

ICRAR, M468, The University of Western Australia, 35 Stirling Highway, Crawley Western Australia, 6009, Australia

Accepted 2015 January. Received 2015 January; in original form 2015 January

ABSTRACT

We conduct the first self-consistent numerical simulations of a recently discovered population of 47 large, faint (ultra-diffuse) galaxies, speculated to lie in the Coma cluster. With structural properties consistent with very large low surface brightness systems (i.e. $\mu(g,0) < 24$ mag arcsec⁻²; r_e comparable to the Galaxy), the red colour ($\langle g-r \rangle \sim 0.8$) and assumed low metallicity of these objects compels us to consider a scenario in which these are underdeveloped galaxies whose early ($z \simeq 2$) accretion to an overdense environment quenched further growth. Our simulations demonstrate the efficacy of this scenario, with respect to available observational constraints, using progenitor galaxy models derived from scaling relations, and idealised tidal/hydrodynamical models of the Coma cluster. The apparent ubiquity of these objects in Coma implies they constitute an important galaxy population; we accordingly discuss their properties with respect to a Λ CDM cosmology, classical LSBs, and the role of baryonic physics in their early formation.

Key words: galaxies: interactions – galaxies: dwarf – galaxies: Magellanic Clouds

1 INTRODUCTION

Low surface brightness galaxies (LSBs) remain an important test for the favoured Λ CDM cosmology, given the dominance of dark matter in these systems whose number density exceeds that of normal galaxies (Bothun, Impey & McGaugh 1997; Dalcanton et al. 1997). Although distinguished by classification from high-SB systems and exhibiting qualitatively different halo properties at low radii (e.g. de Blok, McGaugh & Rubin 2001), their conformance to the Tully-Fisher relation supports a continuity with late-type discs (Zwaan et al. 1995; Schombert & McGaugh 2014). In the standard galaxy formation framework, these diffuse systems nominally formed within low initial density fluctuations (Fall & Efstathiou 1980; Mo, Mao & White 1998), resulting in blue, gas-rich and slowly evolving discs (McGaugh & Bothun 1994). The vulnerability of such tenuous systems to external influence typically precludes their existence in high-density environments (Dekel & Silk 1986; Rosenbaum et al. 2009; Galaz et al. 2011).

Improved imaging techniques reveal however a surprising new population of such galaxies within rich cluster environments. Specifically, we refer to the recent detection

in the Dragonfly Telephoto array of large diffuse galaxies (van Dokkum et al. 2015a, VD15) in the Coma cluster, whose association with the cluster is proposed on the basis of both their spatial distribution and a lower limit on their distance as implied by the unresolved nature of their stellar component. With further examination via high quality CFHT imaging, and assuming a distance equivalent to Coma, the authors assert 47 of these objects as Ultra-diffuse galaxies (UDGs) with effective radii (r_e) ranging from 1.5 to 4.5 kpc, and central surface brightnesses of 24 to 26 mag arcsec⁻² (Table 1). The membership of the largest of these objects in Coma has since been confirmed using spectroscopy from the Keck I telescope (van Dokkum et al. 2015b).

While classical blue LSBs have been previously detected in the Virgo cluster (Impey, Bothun & Malin 1988), the UDGs lie on the faint end of the red sequence of the (more massive) Coma cluster (Gavazzi et al. 2013), a dichotomy possibly related to environmental dependencies. The recent accretion and quenching of gas-rich LSBs in Coma is consistent with 1) the slow formation of LSBs within cosmologically underdense regions; 2) their recent accretion to large-scale structures/filaments (Rosenbaum et al. 2009), and 3) a recent build-up of the faint end/an increase in the dwarf-to-giant ratio in the cluster red sequence since $z = 0.2$ (Lu et al. 2009; Gavazzi et al. 2013). Moreover, other faint dwarves in

^{*} E-mail
kenji.bekki@uwa.edu.au

21101348@student.uwa.edu.au;

Coma display generally radial/anisotropic orbits, suggestive of recent accretion from the field or as part of subgroups (Adami et al. 2009).

If applying stellar population models, however, the median UDG colour $\langle g-r \rangle = 0.8 \pm 0.1$ is consistent with an old stellar disc passively evolving over a timescale up to $z = 2$, if assuming the typically low metallicity of diffuse LSBs (i.e. oxygen abundance $12 + \log(\text{O}/\text{H}) \leq 8$; McGaugh & Bothun 1994). The paucity of quenched field galaxies within this mass range (Geha et al. 2012) thus implies a scenario in which the UDGs were quenched upon infall at high redshift, leading VD15 to speculate that these are examples of failed L_* -type galaxies.

This early quenching is supported by evidence of an almost complete red sequence in a $z = 1.8$ analogue of Coma (JKCS041; Andreon et al. 2014). The apparent absence of UDGs within 300 kpc of the cluster centre, presumably via their destruction here, is also not consistent with their very recent accretion to a kinematically hot host. More generally, the apparent ubiquity of these UDGs in Coma conflicts with the theoretical rarity of large diffuse LSBs such as Malin I (Hoffman, Silk & Wyse 1992), motivating an alternate scenario for their origin.

In this first theoretical study of these objects, we adopt self-consistent numerical methods for hypothetical UDG progenitors to ascertain their evolution within high-density environments modelled on the Coma cluster. Guided by observational constraints from VD15, we devise a theoretical template for the scenario in which these objects are normal galaxies accreted as satellites and quenched soon after the standard epoch of disc formation ($z = 2$). Section 2 describes our UDG model, while Sections 3 and 4 describe its hydrodynamical and tidal interactions within a rich cluster. Section 5 concludes this study with a discussion of these results.

2 A HYPOTHETICAL MODEL FOR A UDG PROGENITOR

Our study adopts a numerical method introduced in Bekki & Couch (2011) and Bekki (2014). The N-body idealisation of the UDG progenitor is constrained by the observed properties (Table 1), in particular the estimated median stellar mass of $6 \times 10^7 M_\odot$, inferred from their median $\langle g-r \rangle$ and a tight mass-colour relation revealed in the GAMA survey.

For an initial stellar (disc) mass (M_d) of $10^8 M_\odot$, abundance matching in cosmological simulations (e.g. Munshi et al. 2013; Behroozi, Wechsler & Conroy 2013) suggest a dark matter (DM) halo mass (M_h , within the virial radius r_{vir}) up to $\sim 10^3 M_d$, although rotation curves obtained from observed samples suggest these simulations produce too much substructure, attaining instead a factor 10 lower prediction (Miller et al. 2014). We adopt an intermediate value for our UDG progenitor, and assume a mean density comparable to the Galaxy (assuming $r_{\text{vir}, \text{MW}} = 258$ kpc and $M_{h, \text{MW}} = 1 \times 10^{12} M_\odot$ Klypin, Zhao & Somerville 2002), giving a r_{vir} of 83 kpc. We assume an exponential disc morphology, with a density defined for the cylindrical radius r and height z :

$$\rho(r, z) \propto \exp\left(-\frac{r}{r_s}\right) \text{sech}^2\left(\frac{z}{0.2r_s}\right).$$

Table 1. Summary of a) properties of observed UDGs b) our reference model parameters

(a) UDG Parameters	Mean (Range)
$\mu(g,0)/\text{mag arcsec}^{-2}$	25 (24-26)
r_e/kpc	3 (1.5-4.5)
Sérsic index, n	1 (0.5-1.5)
Stellar mass, M_s/M_\odot	6×10^7 (1×10^7 - 3×10^8)
Cluster-centric radius/kpc	- (>300)
(b) UDG Model Parameters	Value
N $^\circ$. DM halo particles	1×10^6
N $^\circ$. Stellar particles	3×10^5
N $^\circ$. Gas particles	2×10^5
DM halo mass, $M_h (M_\odot)$	3.2×10^{10}
NFW concentration, c_{NFW}	5.0
DM halo r_{vir} (kpc)	83
Stellar (disc) mass, $M_d (M_\odot)$	10^8
Stellar scalelength, r_d (kpc)	1.7
Stellar scaleheight, z_d (kpc)	0.34
Gas mass, $M_g (M_\odot)$	5×10^8
Gas scalelength, r_g (kpc)	5.1
Gas scaleheight, z_g (kpc)	0.34

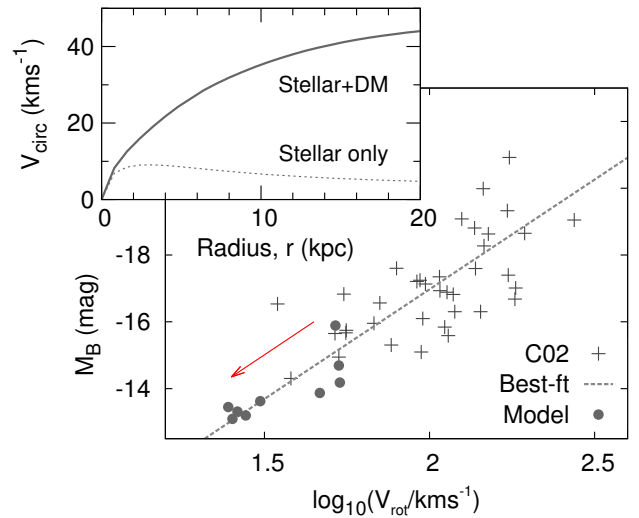


Figure 1. (Top) Initial rotation curve (assuming $V(r) = (GM(<r)/r)^{0.5}$) for the UDG progenitor model; (bottom) simulation BOUND in the V_{rot}/B -band Magnitude phase space (black filled circles); its evolution (with direction highlighted with the red arrow) is consistent with an observed LSB sample (black crosses) with best-fit curve (dashed line), reproduced from Chung et al. (2002).

The scalelength r_s is derived a size-mass $^\alpha$ scaling relation (Dutton & van den Bosch 2009; Ichikawa, Kajisawa & Akhlaghi 2012) whose shallow slope at this stellar mass range ($\alpha \simeq 0.15$, with respect to simple self-similar models based on virial relations where $\alpha \simeq 0.33$) is believed to reflect the role of feedback (Mo, Mao & White 1998; Dekel & Woo 2003; Shen et al. 2003).

Assuming $r_{\text{eff}} = 1.67r_d$, the sizes of the observed UDGs can be attained if we thereafter apply a linear scaling (λ_s) to r_d . If the UDGs are assumed as classical LSBs, λ_s is a proxy

for variations in the initial spin parameter; our adopted $\lambda_s = 1.5$ lies at $\sim 1\sigma$ of typical spin distribution among simulated halos (Maccio et al. 2007), and is consistent with the tendency for high spin halos to host LSB galaxies.

This selection of free parameters (M_d , λ_s) yield a central surface brightness consistent with those observed ($24 < \mu(B,0) / (\text{mag arcsec}^{-2}) < 26$). We further note that the resulting ratio r_e/r_{vir} lies within 1σ of a tight linear relation identified by Kravtsov (2013), consistent with the galaxy size being set by the halo's initial specific angular momentum (Mo, Mao & White 1998).

We adopt the NFW density profile for the halo, defined as:

$$\rho(r) \propto (r/r_h)^{-1} (1 + (r/r_h)^2)^{-1},$$

where $r_h = r_{\text{vir}}/c_{\text{NFW}}$ and c_{NFW} is a concentration factor, here set to 5 in accordance with mass-redshift-dependent relations for the adopted M_d (i.e. Maccio et al. 2007; Munoz-Cuartas et al. 2011). This is similar to the characteristic c_{NFW} among a sample of LSBs obtained from fits to high quality H_α - H_I ($c_{\text{NFW}} \simeq 5 - 6$; McGaugh, Barker & de Blok 2003), although the authors argue that a cored pseudo-isothermal density profile provides a better fit than NFW.

The interstellar medium (ISM) is considered isothermal (temperature 10^4 K), and modelled with smoothed particle hydrodynamics. We assume again an exponential density profile, as for the disc, and adopt a scalelength $r_g = 2.6r_d$ (i.e. the sample mean from Kravtsov 2013), with a total mass (M_g) five times that of the disc, as inferred from scaling relations identified by Popping, Behroozi & Peebles (2015).

Figure 1 illustrates the initial rotation curve of our model (with parameters summarised in Table 1). We do not readily find other curves of comparable extension and V_{rot} in the literature, noting also that, similar to previous simulations of a similar nature (e.g. Kazantzidis et al. 2011), V_{rot} will decline significantly due to substantial mass stripping. The curve is qualitatively similar to LSBs, in which the stellar disc is dynamically insignificant (Bothun, Impey & McGaugh 1997). Our model also lies on the same Tully-Fisher relation exhibited in the sample of LSBs compiled by Chung et al. (2002).

Following the method of Yozin & Bekki (2014), our SF/feedback model (see Bekki 2014, for more detail) is selected principally to avoid gas clumping in the gas-rich ISM while providing the low SF rates of generic LSBs (Schombert, McGaugh & Maciel 2013). To summarise, star formation occurs in the event of a convergent, cool region of gas with local density threshold $> 10^{0.5} \text{ cm}^{-3}$, while the thermal component of Supernova feedback (0.9×10^{51} ergs) is injected into the ISM over an adiabatic expansion timescale of 10^6 yrs.

3 RAM PRESSURE STRIPPING IN A COMA-ANALOGUE CLUSTER

In this section, we test the hypothesis that the UDG progenitor model can be efficiently quenched by ram pressure stripping (RPS) upon first infall and interaction with the intracluster medium (ICM) of a predecessor of

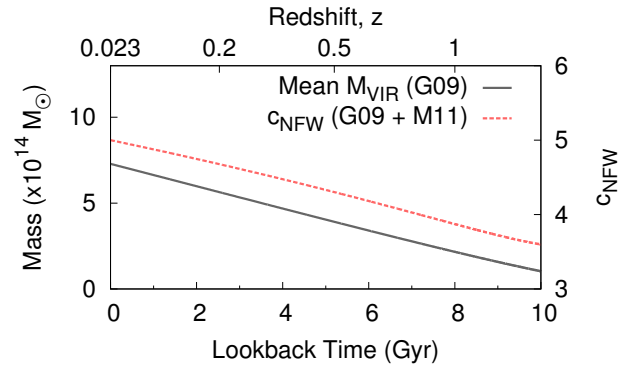


Figure 2. Coma virial mass and concentration, c_{NFW} , as a function of lookback time/ z , as derived from weak lensing methods (Gavazzi et al. 2009) and cosmological simulations (Munoz-Cuartas et al. 2011).

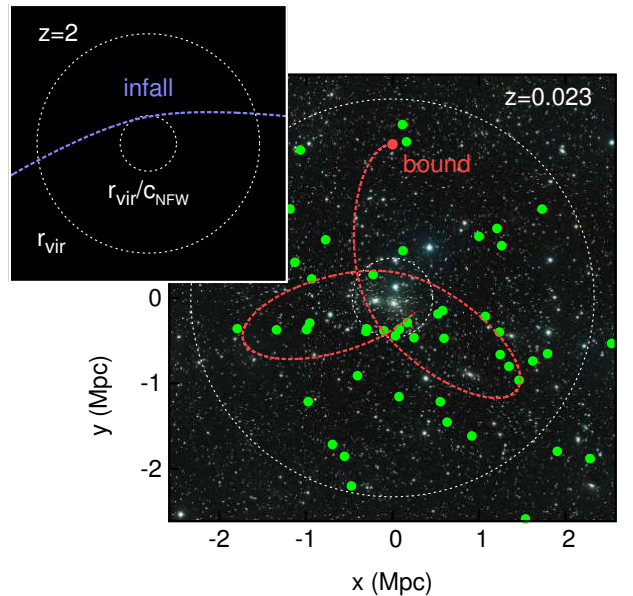


Figure 3. Equal-scale schematics of Coma-cluster models considered in this study, at $z = 0.023$ and $z = 2$ (10 Gyr ago). White dotted lines represent characteristic NFW and virial radii. BOUND and infall orbits are conveyed with dashed lines, overlaid in the $z = 0.023$ case, on an optical image of Coma with green dots showing the locations of observed UDGs (reproduced from van Dokkum et al. 2015a).

Coma at $z = 2$. We derive a model of Coma using recent weak lensing measurements from deep CFHT images, which reveal a dynamical mass M_{coma} (at $z = 0.024$) of $5.1 \times 10^{14} h^{-1} M_\odot$ (Gavazzi et al. 2009). Assuming $H_0 = 70 \text{ km s}^{-1} \text{ Mpc}^{-1}$, this estimate is low compared to previous studies (i.e. Kubo et al. 2007) and is thus conservative within the context of our work. We adopt statistical measures of halo mergers/assembly, followed in cosmological simulations (Fakhouri, Ma & Boylan-Kolchin 2010; Munoz-Cuartas et al. 2011; Ludlow et al. 2013) to attain the evolution of mass and c_{NFW} as a function of redshift, with respect to their present values (Figure 2).

To model the impact of hydrodynamic interactions on our model, we adopt the method of Bekki (2014), in which

a cluster satellite lies within a cubic lattice (with periodic boundary conditions) representing its local ICM. The SPH particles comprising this lattice have their density (and velocity, relative to the fixed satellite) vary according to a cluster-centric radial dependence described by a NFW profile (with c_{NFW} as inferred above). For the extrapolated M_{coma} at $z = 2$, we obtain a total baryonic mass M_{ICM} from Lin et al. (2012), who use X-ray emission to establish $0.1 < M_{\text{ICM}}/M_{\text{coma}} < 0.15$, and an ICM kinetic temperature interpolated from the cluster sample of Matsumoto & Tsuru (2000).

We assume the UDG progenitor is accreted onto the cluster with the cosmologically most common trajectory upon first infall (Benson 2005). Described in terms of the radial/tangential velocity at r_{vir} , this trajectory does not vary significantly since $z = 2$. To avoid setting our satellite in thermal equilibrium with the ICM, the orbit commences at $1.5r_{\text{vir}}$, and is shown schematically in Figure 3.

We find this scenario satisfies the hypothesis that rapid quenching of the UDG progenitor can occur at high z ; their red colour can be facilitated by the drop in the SF rate upon first infall (relative to an isolated counterpart, as illustrated in Figure 4) and consistent with other numerical studies (e.g. Cen, Pop & Bahcall 2014). This occurs in spite of the exclusion, in this simulation, of cluster tides that would otherwise diminish the halo restoring force. While not all gas exceeds escape speed, being retained in the massive halo, its gas surface density is insufficient to permit further SF (generally lying below the typical threshold density for SF of $\sim 10 M_{\odot} \text{pc}^{-2}$). The RP stripped ISM shows a qualitatively similar (jellyfish) morphology to Virgo cluster satellites undergoing a similar process (e.g. Chung et al. 2007).

The uncertainty introduced by the extrapolation of Coma's properties at higher z should be highlighted, given for example, the uncharacteristically high ICM temperature of Coma for its X-ray luminosity (Pimblet, Penny & Davies 2014). Similarly, a recent analysis of the GIMIC cosmological simulations for quenched galaxies residing in ($10^{13-15} M_{\odot}$) host halos illustrates a highly variable RP efficiency with redshift (with primary cause as yet undetermined; Bahe & McCarthy 2015). The authors note, however, that quenched galaxies preferentially lie in overdense regions of the ICM (by a factor 10, with respect to the mean at a given cluster-centric radius; see also Tonnesen & Bryan 2008) in which case our model, devoid of such substructure, can be deemed conservative.

We further emphasise that our model is of similar mass to the dwarf-type model of Bekki (2014), which was also demonstrated to be efficiently quenched in a Coma-type cluster environment during first infall. That his dwarf-type model was HSB, as contrasted with our high spin/diffuse model, would further indicate that the quenching efficiency demonstrated here is not sensitive to our assumptions regarding the construction of the UDG progenitor model.

4 SURVIVAL OF UDG PROGENITORS IN CLUSTER TIDAL ENVIRONMENTS

Our UDG progenitor is hypothesised to reside in Coma over several crossing timescales ($\tau_{\text{cr}} \simeq 1 \text{ Mpc}/1000 \text{ kms}^{-1} \simeq 1 \text{ Gyr}$). Previous studies have highlighted how successive peri-

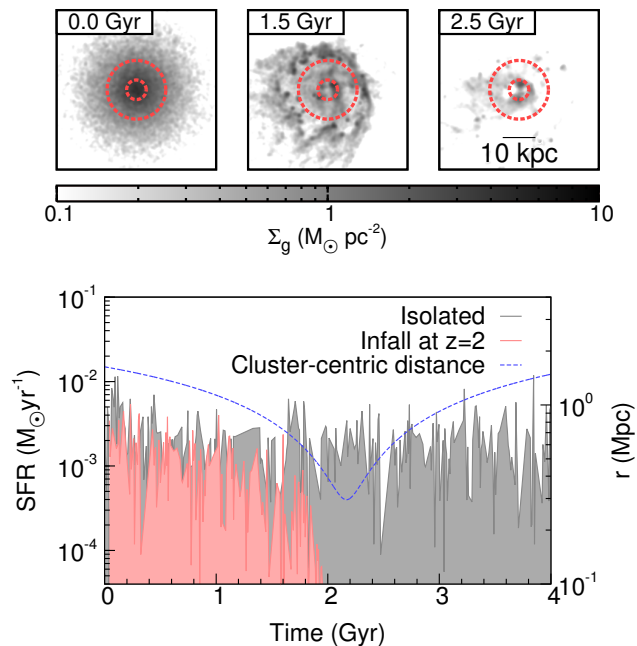


Figure 4. (Top panels) Face-on gas surface mass density distribution for the UDG progenitor during first infall into a Coma-analogue at $z = 2$. The simulation time is denoted at the top left, with effective and optical radii shown with red dotted lines; (bottom) star formation history of the aforementioned simulation (red, with cluster-centric radius shown with the blue dashed line), compared against an isolated example (grey).

centre passages or harassment by other satellites can transform (Sérsic index) $n = 1$ discs to earlier-type morphologies (Moore et al. 1996; Kazantzidis et al. 2011). In this section, we compare the time-evolution of our models structural properties (illustrated in the diagnostic of Figure 5) with observed UDG constraints (Table 1).

The group's tidal influence is modelled explicitly at each simulation time-step with the acceleration imposed upon the constituent stellar/halo particles of the UDG progenitor by the cluster halo's gravitational potential. We adopt the fixed spherically-symmetric NFW profile of Section 3 for the halo mass distribution, and derive the gravitational potential at the location of an individual progenitor particle with its cluster-centric radius.

The trajectory of the progenitor within the cluster potential is defined by a selection of orbits/redshifts. Orbit 'infall' refers again to the cosmologically most common infall trajectory at $z = 2$, adopted in Section 3 (Benson 2005). Orbit 'bound' adopts the $z = 0.023$ properties of Coma, with a ratio of apocentre to pericentre (r_{peri}) set to the median value determined from large-scale simulations (6; e.g. Ghigna et al. 1998), and r_{peri} fixed at 300 kpc, similar to the apparent limit identified by VD15. We accordingly test if UDG progenitors are destroyed below this limit with orbit 'bound' ($< 300 \text{ kpc}$), in which r_{peri} is 150 kpc. We assume that the UDG model would occupy these bound orbits subsequent to its quenching during the initial parabolic orbit 'infall', as a result of dynamical friction experienced through interaction with a live cluster halo (not modelled here).

Figure 5 conveys how, for our initial stellar disc mass $M_{\text{d}} = 10^8 M_{\odot}$, the models following orbits 'bound'

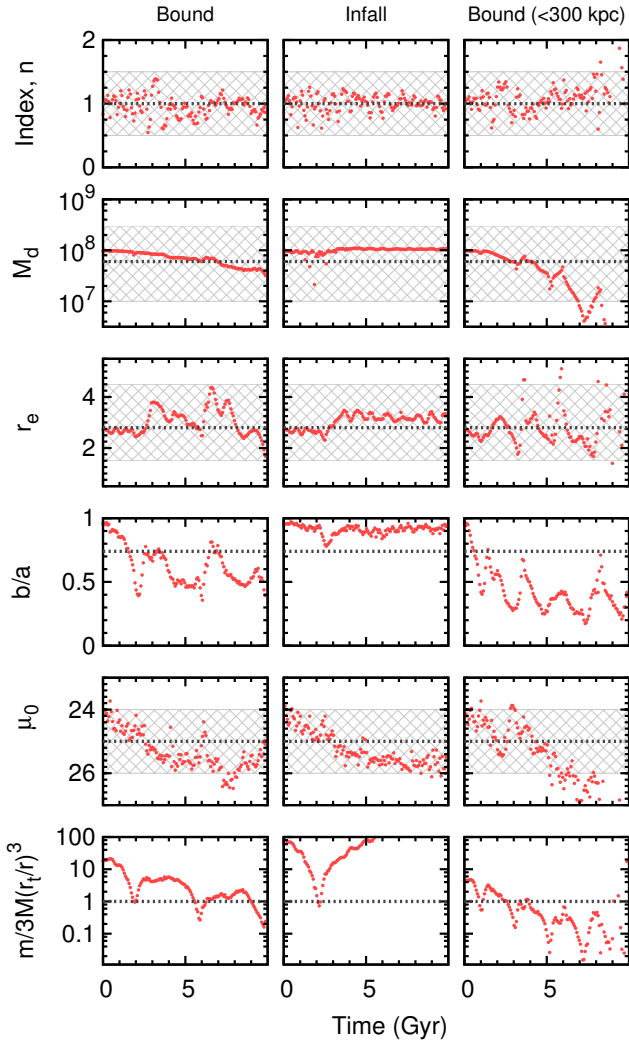


Figure 5. A comparison of parameters from simulations (left to right) ‘bound’, ‘infall’, and ‘bound (<300 kpc)’, against observational constraints (Table 1). From top to bottom: Sérsic index n , stellar mass within g-band limit M_d , effective radius r_e , axial ratio b/a , g-band central surface brightness $\mu(g,0)$, and the ratio of the mass (within r_t) to the mass required to avoid tidal pruning.

and ‘infall’, remain within observed ranges for UDGs. This is in spite of tidal mass loss (estimated from the stellar mass exceeding escape speed) and the passive fading of the stellar disc. We estimate the latter from stellar evolution models (Bruzual & Charlot 2003; Portinari, Sommer-Larsen & Tantaló 2004), assuming an initial stellar metallicity of $0.03 Z_\odot$, comparable to faint Local Group satellites at $z = 2$ (Leaman et al. 2013) and consistent with passive fading since $z = 1 - 2$ to provide the observed $\langle(g-r)\rangle$ colour (VD15).

These models remain disc-like and extended, consistent with VD15 who obtain a good fits in GALFIT for stacked Σ_g/Σ_i images of the UDGs. These, together with deeper imaging and a multicomponent fit of the largest UDG (van Dokkum et al. 2015b), exhibit low n in the range 0.5 to 1.5. Unlike in our similar study, in which $10^9 M_\odot$ dwarf satellites develop strong asymmetries and bulges within a group environment (Yozin & Bekki, in prep.), the disc sta-

bilisation provided by a dominant halo, together with early removal of the ISM, leads to a persistently late-type morphology. These models also tightly match the Tully-Fisher relation, established from a sample of LSBs by Chung et al. (2002), for the duration of their evolution (Figure 1).

The deviations from a unity n are caused principally by elongation of the disc and/or formation of tidal arms. These features are quantified with an axis ratio (b/a) estimated with the μ -weighted mean axial ratio among ellipses fit to isophotes (between the satellites’ central μ and $\mu_g = 28 \text{ mag arcsec}^{-2}$ at $0.25 \text{ mag arcsec}^{-2}$ increments) of the smoothed face-on μ distribution (using a gaussian kernel that matches the $\sim 0.12 \text{ kpc}$ FWHM of the CFHT imaging). The simple morphology of the models (lacking strong bisymmetries like bars due to a low disc mass) means this simple method is sufficiently robust for our purposes, as illustrated in Figure 6. For orbit ‘bound’, which we deem conservative in light of successive r_{peri} at 300 kpc, b/a falls to the lower end permitted by observations (Figure 7); by contrast, ‘infall’ lies at the upper end. This metric alone therefore suggests the UDGs occupy orbits in between these extremes, although we do not account for the effects of their inclination.

For orbit ‘bound (<300 kpc)’, we can demonstrate the effective destruction of the UDG progenitor, denoted by substantial mass loss and disruption to the previously exponential disc, clearly illustrated in mock CFHT images that do not compare well with the observed counterparts (Figure 6). The systems do not, however, resemble the ultra-compact dwarves often found concentrated at their respective cluster centres (Drinkwater et al. 2003). Although occupying a similar magnitude range to the UDGs, the small sizes of UCDs (<100 pc) are speculated to reflect the loss of up to 98 percent of their original luminosity via tidal stripping (Bekki, Couch & Drinkwater 2001).

The bottom row of Figure 5 shows how this satellite disruption is related to an insufficient mass (m_t) enclosed within its tidal radius r_t when interacting with the cluster tidal field at pericentre. For an orbital radius r , tides exerted by the cluster mass M enclosed within r can yield substantial pruning of the satellite if $m_t/(3M(r_t/r)^3) \leq 1$ (Binney & Tremaine 2008). For orbits ‘bound’ and ‘infall’, we find this mass ratio of the order of unity for several τ_{cr} , consistent with their apparent robustness in morphology. Incidentally, we note that VD15 adopt this same formulation to predict, for the UDGs estimated stellar mass, a stellar-halo mass ratio (M_d/M_h) to account for these objects survival at 300 kpc; their value of ~ 0.04 within r_t is consistent with the initial conditions of our progenitor models (Section 2).

5 DISCUSSION AND CONCLUSIONS

Using constraints from the first detections of large faint galaxies (UDGs) in the Coma cluster (VD15), we have developed a theoretical template for their evolutionary history. The exceptionally diffuse stellar component would imply a late infall as deemed common theoretically and observationally among LSBs (Rosenbaum et al. 2009), yet the degeneracy associated with their red colour permits a passive fading since as early as $z = 1 - 2$ (depending on the assumed metallicity). In this context, we have examined the intrigu-

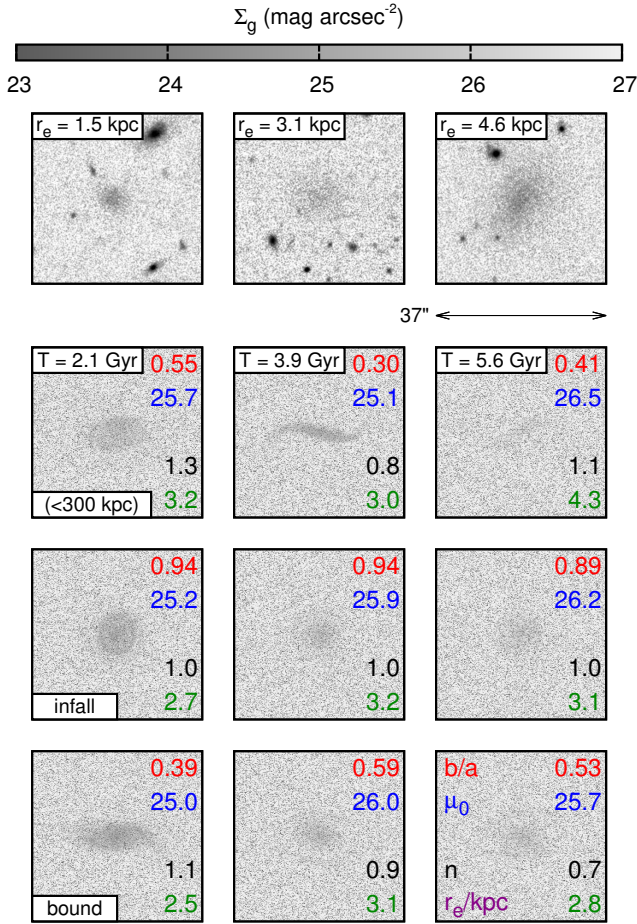


Figure 6. (Top) CFHT imaging of UDGs, illustrating the range in size (reproduced from van Dokkum et al. 2015a); (bottom panels) mock CFHT images (g -band surface brightness) of (from bottom to top) ‘bound’, ‘infall’, and ‘bound (<300 kpc)’, viewed face-on at simulation time ($T =$) 2.1 Gyr (first pericentre passage), 3.9, and 5.6 Gyr (second passage). Coloured labels provide the instantaneous b/a , $\mu(g,0)$, n and r_e .

ing possibility that these UDGs are an example of satellite-quenching at high redshift.

While there are no previous examples of large red LSBs in clusters, the UDGs possess several characteristics (n , $\mu(g,0)$, b/a) similar to Local Group dSphs (VD15). It is intriguing therefore that in an inventory of local resolved stellar populations, the Galactic companions typically formed 30-50 percent of their mass (but in some cases, only 10-20 percent) by $z = 2$ (Weisz et al. 2011). This downsizing (lower mass galaxies showing more prolonged formation epochs) supports the role of reionisation in these objects’ early formation, where gas heating by the UV-background suppresses SF by both preventing gas collapse/accretion and heating the ISM, delaying cooling until $z = 1$ (Babul & Rees 1992; Skillman et al. 2003). The recent finding of a central depression in the surface brightness profile (relative to an exponential disc) of the largest UDG by van Dokkum et al. (2015b), a feature common amongst dSphs, leads them to speculate further the role of early stellar feedback in su-

pressing SF at high- z and contributing to gas loss due to ram pressure stripping (e.g. Stinson et al. 2013).

It remains to be demonstrated if these mechanisms would be efficient for our UDG progenitor (with V_{\max} of 40-50 kms^{-1}), but we note that the construction of our model (Section 2), in particular the choice of λ_s , accommodates the scenario in which the UDGs are underdeveloped HSB galaxies. Since $\log(\lambda_s) \simeq \alpha$, our progenitor model at $z = 2$ can be assumed to have nominally developed a factor ~ 10 more massive stellar disc if not quenched so early.

We presently find tentative support for an early accretion/quenching scenario with the deprojection (with an Abel integral identity) of the UDGs spatial distribution (Figure 7), which reveals a number density (as a function of radius) that can be reasonably fit with a NFW profile with cNFW of 3, consistent with the satellite population at large (Lin, Mohr & Stanford 2004).

If ignoring the small sample size, this implies a relaxed distribution, in a cluster whose two-body relaxation time is of order a Hubble time. However, the more centrally located dwarf satellites of Coma tend to be older (in spite of a wide range of stellar ages depending on the chosen mass proxy; Smith et al. 2012). Figure 7 indicates the 47 known UDGs exhibit no clear trends among their properties as a function of cluster-centric radius, although VD15 note that the intracluster light may be obscuring some UDGs.

Our tidal disruption model is simple, insofar as the tidal harassment from other Coma satellites is not explicitly incorporated (and in which case our mass loss predictions may be lower limits). We have assumed at this stage that the UDGs, as low mass systems in a kinematically hot cluster ($\sigma \simeq 1000 \text{ km s}^{-1}$; Danese, de Zotti & di Tullio 1980), are not significantly disrupted even on long timescales, as demonstrated in previous studies (e.g. Tormen, Diaferio & Syer 1998). In general, dwarf galaxies are weakly influenced by dynamical friction in clusters (i.e. drag force \propto satellite mass), with the associated orbit mostly avoiding regions of strong harassment (Smith, Davies & Nelson 2010). Diffuse systems such as the UDGs may remain quite vulnerable (Moore et al. 1996), but we have tentatively demonstrated here that the halo masses associated with these systems can provide some measure of stability.

We cannot state however if this stability is sufficient in the event that the UDGs were first accreted as part of a group, as exhibited by simulated dwarf satellites (De Lucia et al. 2012). Our models have assumed a static host at the two epochs concerned ($z = 0.023$ and $z = 2$), yet Coma-cluster analogues within cosmological simulations accrete >5 group-mass ($10^{13} M_{\odot}$) halos within the last Gyr alone (Fakhouri, Ma & Boylan-Kolchin 2010). The dynamical state of major subgroups in Coma (e.g. NGC 4839) as pre- or post-merger is uncertain (Burns et al. 1994; Sanders et al. 2013), but the (radial, anisotropic) kinematics of other faint dwarves tentatively suggest a significant recent infall from the field or as part of subgroups (Adami et al. 2009).

Besides pre-processing in the more tidally disruptive environment of a group, tidal interactions between galaxies accreted as a group/filament are also quite feasible (Gnedin 2003). This scenario is not compatible with our hypothesized high- z quenching and low- z late-type morphology of the UDGs, but is consistent with cosmological simula-

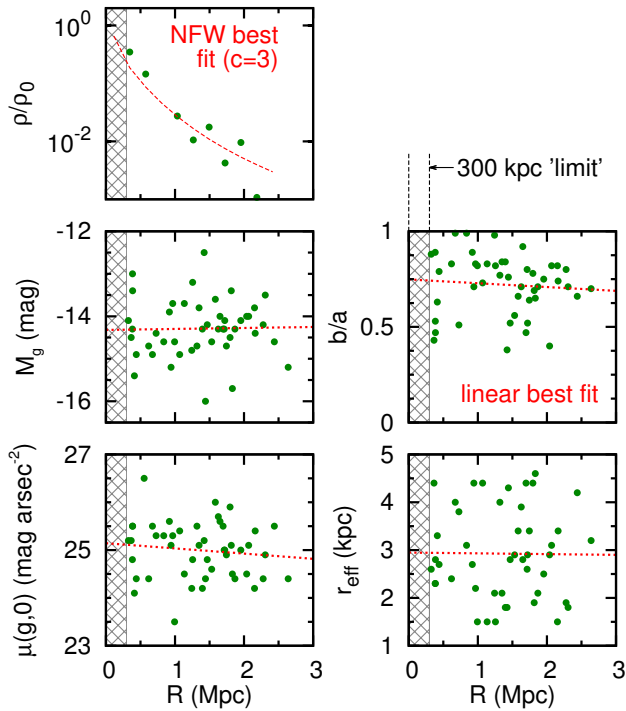


Figure 7. (Top left) Deprojected number density of the 47 detected UDGs (using an Abel integral identity), normalised by the central density of a best-fit NFW profile with c_{NFW} of 3 (see text; red dashed line), as a function of cluster-centric radius; (middle left) g -band Magnitude, (middle right) b/a , (middle left) $\mu(g,0)$, and (middle right) r_e as a function of projected cluster-centric radius for the 47 detected UDGs, with a linear-fit to each data set (red dashed line).

tions which rarely find large intact LSBs in clusters (e.g. Avila-Reese et al. 2005).

To conclude, it is entirely possible that the observed UDGs are classical LSBs, recently accreted, and even on the verge of destruction. The recent deep imaging of the largest UDG evidence does not support its tidal disruption, although this may not be representative of the population (van Dokkum et al. 2015b). We might also speculate if they are the cluster-bound gas-stripped remnants of another population, recently detected in the ALFALFA survey, constituting exceptionally gas-rich (for their stellar mass) dark galaxies, typically with high spin parameters (Huang et al. 2012). The kinematics of the UDGs would certainly aid in identifying their relationship with their hosts' dynamical history e.g. subgroup mergers (Vijayaraghavan, Gallagher & Ricker 2015). With this information, and the dynamical mass/metallicities obtainable in future long-exposure LSB-optimised observations, we look forward to refining our theoretical model.

ACKNOWLEDGEMENTS

We thank the anonymous referee for their comments which improved this paper. We further thank Gerhard Meurer for bringing the original UDG paper to our attention and useful

comments. CY is supported by the Australian Postgraduate Award Scholarship.

REFERENCES

- Adami C., et al., 2009, *A&A*, 507, 1241
 Andreon S., Newman A. B., Trinchieri G., Raichoor A., Ellis R. S., Treu T., 2014, *A&A*, 565, 120
 Avila-Reese V., Colin P., Gottlobber S., Firmani C., Maulbetsch C., 2005, *ApJ*, 634, 51
 Babul A., Rees M. J., 1992, *MNRAS*, 255, 346
 Bahe Y. M., McCarthy I. G., 2015, *MNRAS*, 447, 973
 Behroozi P. S., Wechsler R. H., Conroy C., 2013, *ApJ*, 770, 57
 Bekki K., 2014, *MNRAS*, 438, 444
 Bekki K., Couch W. J., 2011, *MNRAS*, 415, 1783
 Bekki K., Couch W. J., Drinkwater M. J., 2001, *ApJ*, 522, L105
 Benson A. J., 2005, *MNRAS*, 358, 551
 Binney J., Tremaine S., 2008, *Galactic Dynamics*. Princeton University Press, Princeton, NJ
 Bothun G., Impey C., McGaugh S. S., 1997, *PASP*, 109, 745
 Bruzual G., Charlot S., 2003, *MNRAS*, 344, 1000
 Burns J. O., Roettifer K., Ledlow M., Klypin A., 1994, *ApJL*, 427, 87
 Cen R., Pop A. R., Bahcall N. A., 2014, *PNAS*, 111, 7914
 Chung A., van Gorkom J. H., Kenney J. D. P., Vollmer B., 2007, *ApJ*, 659, L115
 Chung A., van Gorkom J. H., O'Neil K., Bothun G. D., 2002, *AJ*, 123, 2387
 Dalcanton J. J., Spergel D. N., Gunn J. E., Schmidt M., Schneider D. P., 1997, *AJ*, 114, 635
 Danese L., de Zotti G., di Tullio G., 1980, *A&A*, 82, 322
 de Blok W. J. G., McGaugh S. S., Rubin V. C., 2001, *AJ*, 122, 2396
 De Lucia G., Weinmann S., Poggianti B. M., Aragón-Salammanca A., Zaritsky D., 2012, *MNRAS*, 423, 1277
 Dekel A., Silk J., 1986, *ApJ*, 303, 39
 Dekel A., Woo J., 2003, *MNRAS*, 344, 1131
 Drinkwater M. J., Gregg M. D., Hilker M., Bekki K., Couch W. J., Ferguson H. C., Jones J. B., Phillipps S., 2003, *Nature*, 423, 519
 Dutton A. A., van den Bosch F. C., 2009, *MNRAS*, 396, 141
 Fakhouri O., Ma C.-P., Boylan-Kolchin M., 2010, *MNRAS*, 406, 2267
 Fall S. M., Efstathiou G., 1980, *MNRAS*, 193, 189
 Galaz G., Herrera-Camus R., Garcia-Lambas D., Padilla N., 2011, *ApJ*, 728, 74
 Gavazzi R., Adami C., Durret F., Cuillandre J., Ilbert O., Mazure A., Pello R., Ulmer M. P., 2009, *A&A*, 498, L33
 Gavazzi R., et al., 2013, *A&A*, 553, A90
 Geha M., Blanton M. R., Yan R., Tinker J. L., 2012, *ApJ*, 757, 1
 Ghigna S., Moore B., Governato F., Lake G., Quinn T., Stadel J., 1998, *MNRAS*, 300, 146
 Gnedin O. Y., 2003, *ApJ*, 582, 141
 Hoffman Y., Silk J., Wyse R. F. G., 1992, *ApJL*, 388, 13
 Huang S., Haynes M. P., Giovanelli R., Brinchmann J., 2012, *ApJ*, 756, 113
 Ichikawa T., Kajisawa M., Akhlaghi M., 2012, *MNRAS*, 422, 1014
 Impey C., Bothun G., Malin D., 1988, *ApJ*, 330, 634
 Kazantzidis S., Lokas E. L., Callegari S., Mayer L., Moustakas L. A., 2011, *ApJ*, 726, 2
 Klypin A., Zhao H., Somerville R. S., 2002, *ApJ*, 573, 597
 Kravtsov A. V., 2013, *ApJL*, 764, 31
 Kubo J. M., Stebbins A., Annis J., Dell'Antonio I. P., Lin H., Khiabani H., Frieman J. A., 2007, *ApJ*, 671, 1466
 Leaman R., et al., 2013, *ApJ*, 767, 131
 Lin Y.-T., Mohr J. J., Stanford S. A., 2004, *ApJ*, 610, 745

- Lin Y.-T., Stanford S. A., Eisenhardt P. R. M., Vikhlinin A., Maughan B. J., Kravtsov A., 2012, *ApJL*, 745, L3
- Lu T., Gilbank D., Balogh M., Bognat A., 2009, *MNRAS*, 399, 1858
- Ludlow A. D., et al., 2013, *MNRAS*, 432, 1103
- Maccio A. V., Dutton A. D., van den Bosch F. C., Moore B., Potter D., Stadel J., 2007, *MNRAS*, 378, 55
- Matsumoto H., Tsuru T. G., 2000, *PASJ*, 52, 153
- McGaugh S. S., Barker M. K., de Blok W. J., 2003, *ApJ*, 584, 566
- McGaugh S. S., Bothun G. D., 1994, *AJ*, 107, 530
- Miller S. H., Ellis R. S., Newman A. B., Benson A., 2014, *ApJ*, 782, 2
- Mo H. J., Mao S., White S. D. M., 1998, *MNRAS*, 295, 319
- Moore B., Katz N., Lake G., Dressler A., Oemler A., 1996, *Nature*, 379, 613
- Munoz-Cuartas J. C., Maccio A. V., Gottlober S., Dutton A. A., 2011, *MNRAS*, 584, 94
- Munshi F., et al., 2013, *ApJ*, 766, 56
- Pimblet K. A., Penny S. J., Davies R. L., 2014, *MNRAS*, 438, 3049
- Popping G., Behroozi P. S., Peebles M. S., 2015, *MNRAS*, 449, 477
- Portinari L., Sommer-Larsen J., Tantalo R., 2004, *MNRAS*, 347, 691
- Rosenbaum S. D., Krusch E., Bomans D. J., Dettmar R.-J., 2009, *A&A*, 504, 807
- Sanders J. S., Fabian A. C., Churazov E., Schekochihin A. A., Simionescu A., Walker S. A., Werner N., 2013, *Science*, 341, 1365
- Schombert J., McGaugh S., 2014, *PASA*, 31, 11
- Schombert J., McGaugh S., Maciel T., 2013, *AJ*, 146, 41
- Shen S., et al., 2003, *MNRAS*, 343, 978
- Skillman E. D., Tolstoy E., Cole A. A., Dolphin A. E., Saha A., Gallagher J. S., Dohm-Palmer R. C., Mateo M., 2003, *ApJ*, 596, 2535
- Smith R., Davies J. I., Nelson A. H., 2010, *MNRAS*, 405, 1723
- Smith R. J., Lucey J. R., Price J., Hudson M. J., 2012, *MNRAS*, 434, 1964
- Stinson G. S., Brook C., Macció A. V., Wadsley J., Quinn T. R., Couchman H. M. P., 2013, *MNRAS*, 428, 129
- Tonnesen S., Bryan G. L., 2008, *ApJ*, 684, L9
- Tormen G., Diaferio A., Syer D., 1998, *MNRAS*, 299, 728
- van Dokkum P. G., Abraham R., Merritt A., Zhang J., Geha M., Conroy C., 2015a, *ApJL*, 798, L45
- van Dokkum P. G., et al., 2015b, *ApJL*, 804, L26
- Vijayaraghavan R., Gallagher J. S., Ricker P. M., 2015, *MNRAS*, 447, 3623
- Weisz D. R., et al., 2011, *ApJ*, 739, 5
- Yozin C., Bekki K., 2014, *MNRAS*, 439, 1948
- Zwaan M. A., van der Hulst J. M., de Blok W. J. G., McGaugh S. S., 1995, *MNRAS*, 273, L35

This paper has been typeset from a $\text{\TeX}/\text{\LaTeX}$ file prepared by the author.